Inelastic light scattering by collective charge-density excitations in GaAs-$Ga_{1-x}Al_xAs$ superlattices

G. Eliasson, P. Hawrylak, and J. J. Quinn
Department of Physics, Brown University, Providence, Rhode Island 02912
(Received 17 October 1986)

We consider the collective excitations of a finite GaAs-$Ga_{1-x}Al_xAs$ superlattice with arbitrary subband structure and electronic density. The density-density correlation function is calculated with use of the random-phase approximation, augmented by the local-density-functional theory. Exchange and correlation effects, self-consistent subband wave functions and energies, and intersubband scattering for arbitrary electron densities are taken into account. The resonant inelastic-light-scattering spectra by collective excitations are calculated. It is found that coupling between intersubband and intrasubband modes is very important when several subbands are occupied, in contrast to the results obtained with only a single subband occupied. The effects of exchange and correlation are found to be small.

I. INTRODUCTION

The development of advanced growth techniques such as molecular-beam epitaxy (MBE), has made it possible to produce a variety of semiconductor superlattices.[1] Most of the experimental and theoretical work has been focused on either GaAs-$Ga_{1-x}Al_xAs$ superlattices (type-I superlattices), or on GaSb-InAs superlattices (type II). A type-I superlattice consists of an array of quasi-two-dimensional electron gases, while a type-II superlattice consists of alternating electron and hole layers. The rich spectrum of single-particle and collective excitations (plasmons) in superlattices have primarily been studied using inelastic light scattering (Raman scattering).[2-6] The single-particle and plasmon spectra are distinguished by the polarization of the scattered light with respect to the incident light.[7] As a result of these experiments, numerous theoretical works have been published on plasmons in superlattices[8-11] and on the theory of inelastic light scattering by collective excitations. Jain and Allen[12] have calculated Raman intensities from semi-infinite and finite arrays of two-dimensional electron gas layers. Katayama and Ando[13] and King-Smith and Inkson[14] included minibands in a self-consistent calculation for an infinite superlattice, thereby neglecting surface effects. An intermediate approach was used by Hawrylak, Wu, and Quinn[15] who included subband structure in the so-called diagonal approximation, for a semi-infinite superlattice. The diagonal approximation means that coupling between intrasubband and intersubband excitations is neglected.[8,15] It is known to work well for a system where only the first subband is occupied by electrons in equilibrium. However, most systems that have been produced and studied experimentally, have the two lowest subbands occupied, and for such systems, coupling between the different plasmons is expected to be more important, especially when the intersubband separation is of the same order as the three-dimensional plasma frequency. The light scattering experiments have been interpreted qualitatively using a simple layered electron gas model. This model obviously neglects all of the effects discussed above, and it is therefore desirable to test the applicability of this model to real superlattices. This can only be done by more elaborate calculations.

In passing, we note that in the case of a type-II superlattice, calculations on finite systems of two-dimensional layers of electrons and holes have been done by Tzoar and Zhang,[16] and by us.[17] We also included the effect of subbands in the diagonal approximation.

In this paper we present a theory of collective excitations in a finite type-I superlattice, including intersubband scattering, self-consitent electronic wave functions, and exchange-correlation effects in the calculation. (A shorter version of this paper was presented at the 18th International Conference on the Physics of Semiconductors, Stockholm 1986.) We have also calculated the Raman intensity for such a system. The results are compared with simple, approximate calculations. The theory is illustrated by a system where the intersubband separation is small compared to the intrasubband plasmon frequency, and the effect of intersubband scattering is important.

II. THE MODEL

The system consists of N quantum wells embedded in a medium with dielectric constant ϵ, occupying the space $z > -\delta$. The other half-space is filled by an insulator with a constant ϵ_0. The wells are centered at $z = la$, $l = 0, 1, \ldots, N-1$, and have width L. The single-particle states are assumed to be of the form

$$|q,l,m\rangle = e^{i\mathbf{q}\cdot\mathbf{r}}\xi_m(z-la)\ ,$$

where m is the subband index and $\mathbf{q}$ is the momentum in the plane perpendicular to the z axis. We assume that the

electrons are localized in the wells (flat minibands), and we perform all calculations at zero temperature. The $Ga_{1-x}Al_xAs$ layers are modeled as a potential barrier with height $V_0=100x$ meV and width $d_1=a-L$, where x is the partial fraction of Al. The ionized donors inside the barriers are replaced by a uniform positive background. The doped regions are separated from the GaAs wells by undoped layers of thickness d_2. The wave functions are calculated using a self-consistent Hartree approximation with an exchange-correlation potential. This method is well described by Ando and Mori,[18] but for completeness we give a brief outline in Appendix A.

III. DENSITY-DENSITY CORRELATION FUNCTION

The density-density correlation function $\Pi(q,\omega,z,z')$ for a semi-infinite type-I superlattice has been calculated by Jain and Allen[12] and by us.[15] It has also been recently calculated for a type-II superlattice by Tzoar and Zhang[16] and by us.[17]

In this paper we will assume that more than one subband is occupied, the case where intersubband scattering turns out to be crucial.

Following Ref. 14 we expand the density-density correlation function in the single-particle states

$$\Pi(q,\omega,z,z')=\sum_{l,l'}\sum_{m,n}\sum_{m',n'}\Pi_{mn,m'n'}(l,l')\xi_m(z-la)\xi_n(z-la)\xi_{m'}(z'-l'a)\xi_{n'}(z'-l'a)\ . \tag{3.1}$$

In the random-phase approximation (RPA), $\Pi(q,\omega,z,z')$ satisfies the equation

$$\Pi_{mn,m'n'}(l,l')=\Pi^0_{mn}\delta_{mn'}\delta_{nm'}\delta_{ll'}+\Pi^0_{mn}\sum_{l''}\sum_{m'',n''}V_{mn,m''n''}(l,l'')\Pi_{m''n'',m'n'}(l'',l')\ . \tag{3.2}$$

Π^0_{mn} is the polarizability of the noninteracting system,[8,19] and is given by

$$\Pi^0_{mn}=2\int\frac{d^2k}{(2\pi)^2}\frac{f(\varepsilon_{n,\mathbf{k}+\mathbf{q}})-f(\varepsilon_{m,\mathbf{k}})}{\varepsilon_{n,\mathbf{k}+\mathbf{q}}-\varepsilon_{m,\mathbf{k}}-\hbar\omega-i\delta}\ . \tag{3.3}$$

$V_{mn,m'n'}(l,l')$ is the electron-electron interaction:

$$V_{mn,m'n'}(l,l')=V_q\int dz\int dz'\,\xi_m(z-la)\xi_n(z-la)(e^{-q|z-z'|}+\alpha e^{-q(z+z')})\times\xi_{m'}(z'-l'a)\xi_{n'}(z'-l'a)+\delta_{l,l'}\int dz\,\xi_m(z)\xi_n(z)U_{\rm xc}(z)\xi_{m'}(z)\xi_{n'}(z)\ , \tag{3.4}$$

where $V_q=2\pi e^2/\epsilon q$ and $\alpha=e^{-2\delta q}(\epsilon-\epsilon_0)/(\epsilon+\epsilon_0)$. $U_{\rm xc}(z)$ is the functional derivative of the exchange-correlation potential with respect to the local density $n(z)$ of electrons

$$U_{\rm xc}(z)=\frac{\delta V_{\rm xc}[n]}{\delta n(z)}\ . \tag{3.5}$$

This approximation is equivalent to the static vertex correction.[18] In order to reduce the size of the matrix $\Pi_{mn,m'n'}(l,l')$ we can symmetrize Π in the indices by defining χ as

$$\chi_{mn,m'n'}=\begin{cases}\Pi_{mm,m'm'}, & \text{if } m=n,\ m'=n'\ ,\\ \Pi_{mm,m'n'}+\Pi_{mm,n'm'}, & \text{if } m=n,\ m'\neq n'\ ,\\ \Pi_{mn,m'm'}+\Pi_{nm,m'm'}, & \text{if } m\neq n,\ m'=n'\ ,\\ \Pi_{mn,m'n'}+\Pi_{nm,m'n'}+\Pi_{mn,n'm'}+\Pi_{nm,n'm'}, & \text{if } m\neq n,\ m'\neq n'\ .\end{cases} \tag{3.6}$$

$$\chi^0_{mn}=\begin{cases}\Pi^0_{mm}, & \text{if } m=n\ ,\\ \Pi^0_{mn}+\Pi^0_{nm}, & \text{if } m\neq n\ .\end{cases} \tag{3.7}$$

χ obeys then the equation

$$\chi_{mn,m'n'}(l,l')=\chi^0_{mn}\delta_{mm'}\delta_{nn'}\delta_{ll'}+\chi^0_{mn}\sum_{l''}\sum_{m''\le n''}V_{mn,m''n''}(l,l'')\chi_{m''n'',m'n'}(l'',l')\quad m\le n \text{ and } m'\le n'\ . \tag{3.8}$$

From the definition of χ, it is clear the χ is symmetric under $m\leftrightarrow n$ and $m'\leftrightarrow n'$. We can write $\chi_{mn,m'n'}(l,l')$ as a matrix $\chi_{pp'}=\underline{\chi}$ where the composite index p only includes those (m,n) for which $m\le n$. In a quantum well with four subbands, $\Pi_{mn,m'n'}$ is a 16×16 matrix, and $\underline{\chi}$ a 10×10 matrix. In matrix form, Eq. (3.8) is then

$$\underline{\chi}(l,l')=\underline{\chi}^0\delta_{ll'}+\underline{\chi}^0\cdot\sum_{l''}\underline{V}(l,l'')\cdot\underline{\chi}(l'',l')\ . \tag{3.9}$$

As in previous papers, we now Fourier transform all quantities,[12,15,17] e.g.,

$$\underline{\chi}(k,k')=\frac{1}{N}\sum_{l,l'=0}^{N-1}e^{-ikla}\underline{\chi}(l,l')e^{ik'l'a}\ , \tag{3.10}$$

$$\underline{\chi}(l,l')=\frac{1}{N}\sum_{k,k'} e^{ikla}\underline{\chi}(k,k')e^{-ik,l'a} , \tag{3.11}$$

where $k=2\pi\pi n/aN$, $n=1,2,\ldots,N$. The Fourier transform of Eq. (3.9) is then

$$\underline{\chi}(k,k')=\underline{\chi}^0\delta_{k,k'}+\underline{\chi}^0\cdot\sum_{k''}\underline{V}(k,k'')\cdot\chi(k'',k') . \tag{3.12}$$

We now decompose $\underline{V}$ and $\underline{\chi}$ into a part diagonal in k,k', called the bulk part, and the rest, called the surface part:

$$\underline{V}=\underline{V}_B(k)\delta_{k,k'}+\underline{V}_S(k,k') , \tag{3.13}$$

$$\underline{\chi}=\underline{\chi}_B(k)\delta_{k,k'}+\underline{\chi}_S(k,k') . \tag{3.14}$$

Equation (3.12) can now be solved to give

$$\underline{\chi}_B(k)=[\underline{1}-\underline{\chi}^0\cdot\underline{V}_B(k)]^{-1}\cdot\chi^0 , \tag{3.15}$$

$$\chi_S(k,k')=\frac{1-e^{-qaN}}{4NP(k)P(k')}\underline{\chi}_B(k)\times(\underline{A}-\underline{B}_1e^{ika}-\underline{B}_2e^{-ik'a}+\underline{C}e^{i(k-k')a})\times\underline{\chi}_B(k') , \tag{3.16}$$

where $P(k)=\cosh(qa)-\cos(ka)$. $\underline{A}$, $\underline{B}_1$, $\underline{B}_2$, and $\underline{C}$ are the solutions to

$$M\cdot\begin{bmatrix}\underline{A}\\ \underline{B}_1\end{bmatrix}=\begin{bmatrix}\underline{a}\\ \underline{b}_1\end{bmatrix},\quad M\cdot\begin{bmatrix}\underline{B}_2\\ \underline{C}\end{bmatrix}=\begin{bmatrix}\underline{b}_2\\ \underline{c}\end{bmatrix} , \tag{3.17}$$

and $\underline{a}$, $\underline{b}_1$, $\underline{b}_2$, $\underline{c}$, and M are given in Appendix B.

The poles of $\underline{\chi}(l,l')$ define the collective excitations of the system. $\underline{\chi}$ is also very useful for calculating intensities of ineleastic light scattering (Raman scattering), electron-energy-loss (EEL) spectra,[20] impurity screening,[21] and the lifetime of excited states.[22] The expression for the Raman intensity has been derived before, so we will only give the result.[7,12,15,17] If the incoming and scattered light have frequencies and wave vectors $(\omega_i,\mathbf{q}_i,k_z^i)$ and $(\omega_s,\mathbf{q}_s,-k_z^s)$, then the Raman intensity is proportional to

$$F(\omega,\mathbf{Q})=\int dz\int dz'\,e^{-ik_z^*z}e^{ik_zz'}\mathrm{Im}[-\Pi(q,\omega,z,z')] , \tag{3.18}$$

where

$$\omega=\omega_i-\omega_s ,$$

$$\mathbf{Q}=(\mathbf{q},k_z)=(\mathbf{q}_i-\mathbf{q}_s,k_z^i+k_z^s) .$$

Using the approximation

$$k_z^i=k_z^s=k+\frac{i}{2\lambda} ,$$

where

$$k=\frac{\omega_i}{c}\mathrm{Re}\sqrt{\epsilon} ,$$

$$\frac{1}{\lambda}=\frac{2\omega_i}{c}\mathrm{Im}\sqrt{\epsilon} ,$$

we can write function $F(\omega,\mathbf{Q})$ as

$$F(\omega,\mathbf{Q})=-\sum_{l,l'}\mathbf{A}(l)\cdot\mathrm{Im}[\underline{\chi}(l,l')]\cdot\mathbf{A}^*(l') , \tag{3.19}$$

where

$$A_p(l)=\int dz\,e^{-2ikz}e^{-z/\lambda}\xi_m(z-la)\xi_n(z-la) . \tag{3.20}$$

$2k$ is thus the momentum transfer to the plasmon from a photon along the superlattice axis, and λ is the photon decay length inside the material. λ is responsible for broadening of the peak. We also introduce a finite lifetime of the excitations by letting $\omega\to\omega+i\gamma_e$ in the expression for χ^0.

IV. RESULTS

First we apply the theory to a GaAs-$Ga_{1-x}Al_xAs$ sample studied experimentally by Olego *et al.*[2] and theoretically by several groups.[12,13] The parameters for this sample are $L=260$ Å, $a=890$ Å, $d_2=150$ Å, $n_s=7.3\times10^{11}$ cm^{-2}, $V_0=200$ MeV, $\delta=0.2a$, $N=20$. For GaAs we use $m=0.068m_e$, and

$$\epsilon(\omega)=\epsilon_\infty\frac{\omega^2-\omega_{\mathrm{LO}}^2+i\gamma_{\mathrm{ph}}\omega}{\omega^2-\omega_{\mathrm{TO}}^2+i\gamma_{\mathrm{ph}}\omega}$$

with $\epsilon_\infty=11.1$, $\hbar\omega_{\mathrm{LO}}=36.7$ meV, $\hbar\omega_{\mathrm{TO}}=33.6$ meV. The self-consistent calculation gives $E_F=18.9$ meV and $E_{01}=12.2$ meV, so the two lowest subbands are occupied. Figure 1 shows the Raman intensity for the intrasubband plasmon for $qa=0.43$, $2ka=0.5$, $\gamma_e=\gamma_{\mathrm{ph}}=0.3$ meV. (The experiment of Olego *et al.* had $2ka=4.94$. With our choice of k, the discrete nature of the plasmon is more visible.) Jain and Allen found that this system can be fit very well by a model neglecting subband structure all together, i.e., a layered electron-gas model (LEG). To understand this result we compare our results with LEG calculations: the solid line is a calculation using self-consistent wave functions and the dashed line the layered electron gas calculation. The agreement is quite good. It is due to intersubband scattering, which becomes impor-

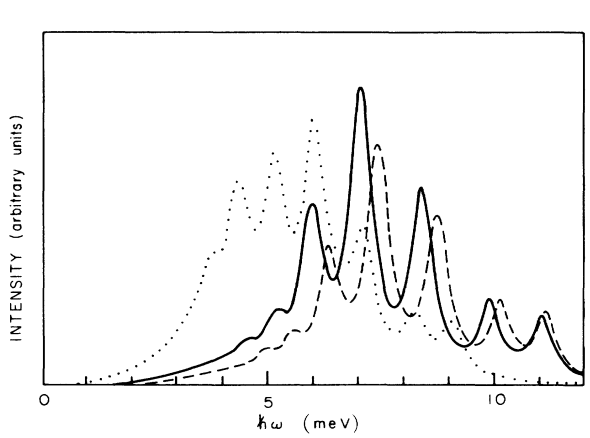

FIG. 1. Intrasubband peak for a system with the parameters $n_s=7.3\times10^{11}$ cm^{-2}, $a=890$ Å, $L=250$ Å, $qa=0.43$, $N=20$, $2ka=0.5$. Solid line is self-consistent calculation, dashed line layered two-dimensional (2D) electron gas, dotted line diagonal approximation.

tant when more then one subband is occupied. This is illustrated by the dotted line in Fig. 1 where intersubband scattering is neglected, i.e., only the diagonal elements of $\underline{\chi}$ are kept. A simple two-band model reveals the mechanism: In the diagonal approximation the upper part of the diagonal matrix $\underline{\epsilon}(k)=\underline{1}-\underline{V}_B(k)\cdot\underline{\chi}^0$ is, using long wavelength expressions for $\underline{\chi}^0$, and neglecting exchange and correlation:

$$\underline{\epsilon}(k)=\begin{bmatrix} 1-\frac{\omega_{00}^2}{\omega^2} & 0 & 0 \\ 0 & 1-\frac{\omega_D^2}{\omega^2-E_{01}^2} & 0 \\ 0 & 0 & 1-\frac{\omega_{11}^2}{\omega^2} \end{bmatrix}, \tag{4.1}$$

where

$$\omega_{ii}=\frac{2\pi e^2 n_i}{\epsilon}\frac{q^2 a_i}{1-\cos(ka)},\quad i=0,1\ , \tag{4.2}$$

$$n_0=n_s\frac{E_F}{2E_F-E_{01}}\ , \tag{4.3}$$

$$n_1=n_s\frac{E_F-E_{01}}{2E_F-E_{01}}\ , \tag{4.4}$$

$$\omega_D^2=\frac{2\pi e^2 n_s}{\epsilon}\frac{E_{01}}{2E_F-E_{01}}L_{01,01}\ , \tag{4.5}$$

$$a_i=a+L_{ii,ii}[1-\cos(ka)]\ , \tag{4.6}$$

$$L_{mn,m'n'}=-\int dz\int dz'\,\xi_m(z)\xi_n(z)\,|z-z'|\times\xi_{m'}(z')\xi_{n'}(z')\ . \tag{4.7}$$

n_0 and n_1 are the densities of electrons in the first and second subband, respectively. ω_{ii} is the frequency of the bulk intrasubband plasmon of a system with n_i electrons per well, and ω_D is the depolarization shift of the intersubband plasmon.[8] The dispersion relation $\det\underline{\epsilon}(k)=0$ gives the intersubband mode $\omega=\omega_{01}=(\omega_D^2+E_{01}^2)^{1/2}$, and *two* intrasubband modes; $\omega=\omega_{00}$ and $\omega=\omega_{11}$ for $q\to 0$. However, when two subbands are occupied, some off-diagonal elements are of $O(1)$ as $q\to 0$. To $O(q^2)$ $\underline{\epsilon}(k)$ is for a symmetric quantum well (approximating $a_i\simeq a$)

$$\underline{\epsilon}(k)=\begin{bmatrix} 1-\frac{\omega_{00}^2}{\omega^2} & -i\frac{2\pi e^2}{\epsilon}\frac{2n_s E_{01}^*}{\omega^2-E_{01}^2}sz_{01} & -\frac{\omega_{11}^2}{\omega^2} \\ i\frac{2\pi e^2}{\epsilon}\frac{n_0 q^2}{m\omega^2}sz_{01} & 1-\frac{\omega_D^2}{\omega^2-E_{01}^2} & -i\frac{2\pi e^2}{\epsilon}\frac{n_1 q^2}{m\omega^2}sz_{01} \\ -\frac{\omega_{00}^2}{\omega^2} & i\frac{2\pi e^2}{\epsilon}\frac{2n_s E_{01}^*}{\omega^2-E_{01}^2}sz_{01} & 1-\frac{\omega_{11}^2}{\omega^2} \end{bmatrix}, \tag{4.8}$$

where

$$E_{01}^*=\frac{E_{01}^2}{2E_F-E_{01}}\ , \tag{4.9}$$

$$z_{01}=\int dz\,\xi_0(z)z\xi_1(z)\ , \tag{4.10}$$

$$s=\frac{\sin(ka)}{1-\cos(ka)}\ . \tag{4.11}$$

The dispersion relation is now

$$\omega^6-\omega^4(\omega_{01}^2+\omega_p^2)+\omega^2(\omega_{01}^2\omega_P^2-2\omega_P^2\delta)+\omega_P^6\varphi=0\ , \tag{4.12}$$

where

$$\omega_P^2=\frac{2\pi e^2 n_s}{\epsilon}\frac{q^2 a}{1-\cos(ka)}\ , \tag{4.13}$$

$$\delta=\frac{1}{2\omega_P^4}(\omega_{I1}^4+\omega_{I0}^4)\ , \tag{4.14}$$

$$\omega_{I0,1}^2=\frac{2\pi e^2 q}{\epsilon}(2n_s E_{01}^* n_{0,1}/m)^{1/2}\,|sz_{01}|\ , \tag{4.15}$$

$$\varphi=\frac{1}{\omega_P^6}(\omega_{11}^2\omega_{I0}^4+\omega_{00}^2\omega_{I1}^4)\ . \tag{4.16}$$

Assuming that $\delta,\varphi\ll 1$ and $\omega_{01}\gg\omega_P$ we can put $\omega=\omega_P(1+\gamma)$, $\gamma\ll 1$, which gives us

$$\gamma=\frac{\omega_P^2}{\omega_P^2-\omega_{01}^2}(2\delta-\varphi)\ ,$$

i.e., one intrasubband mode near ω_P, the value a layered electron gas model would give. The other mode is now unphysical ($\omega^2<0$). This means that electrons in both subbands contribute to the intrasubband plasmon. The diagonal approximation is no longer valid while the more intuitive picture of the layered electron gas with the total electron density works well for intrasubband modes.

A situation where intersubband scattering becomes very important occurs when the energies of the intrasubband and intersubband plasmons are of the same order. Figure 2 shows ω versus q for such a system. The parameters are $L=320$ Å, $a=980$ Å, $d_2=150$ Å, $n_s=8.2\times10^{11}$ cm^{-2}, $N=6$. The calculated Fermi energy and subband separation are $E_F=17.6$ meV and $E_{01}=6.3$ meV, respectively. One observes the crossing of intersubband and intrasubband modes. The shaded area represents single-particle intersubband excitations. One expects the intrasubband

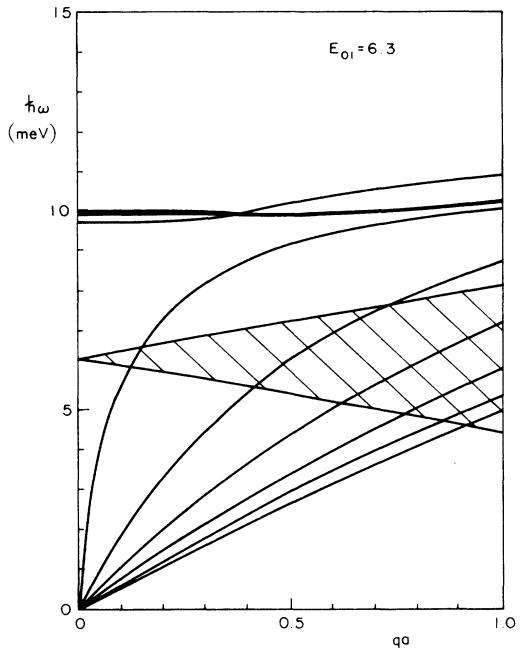

FIG. 2. Dispersion relation ω vs q for a superlattice with six quantum wells. The parameters are $n_s=8.2\times10^{11}$ cm^{-2}, $a=980$ Å, $L=310$ Å, $d_2=150$ Å, $\delta=0.6a$. The intersubband separation is 6.3 meV. The dashed area is the allowed region for intersubband single-particle excitations. Due to the relatively weak coupling between intersubband and intrasubband plasmons in this region, the intrasubband modes do not experience any significant Landau damping.

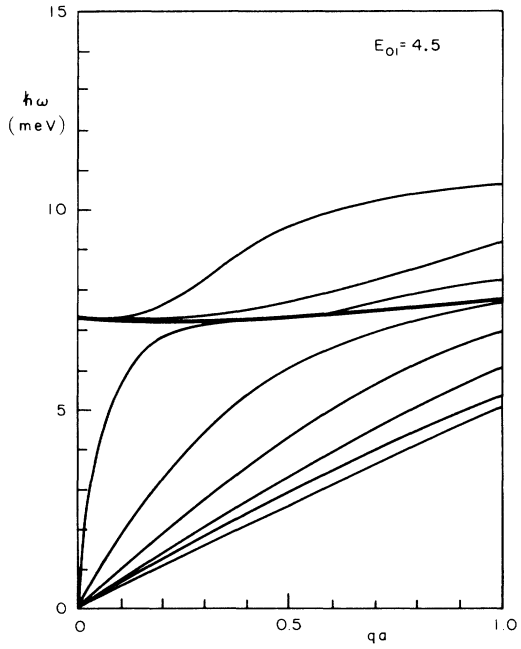

FIG. 3. Dispersion relation ω vs q for a system with the same parameters as in Fig. 2, except that $L=350$ Å. The intersubband separation now becomes 4.5 meV.

plasmons to be damped in this region. However, the coupling between intrasubband and intersubband plasmons is too weak to give any significant decay of intrasubband modes into single-particle intersubband excitations.

A more pronounced crossing is shown in Fig. 3. The system here has the same parameters as in Fig. 2, except that $L=350$ Å. This gives $E_F=16.7$ meV and $E_{01}=4.5$ meV. More modes are crossing, since the intrasubband modes are lower in energy. A detail of the crossing is shown in Fig. 4, for the $ka=0.5$ bulkmode (infinite system) of the system in Fig. 3.

The exchange-correlation potential reduces the energies of the modes. For the system in Fig. 1 we find a shift of ~0.5 meV for intrasubband modes, while the system in Fig. 3 experiences a shift of ~0.2 meV. In the case of intersubband modes the shift, which is also called excitonic shift, is about 0.8 meV for the system in Fig. 1, and 0.3 meV for the system in Fig. 3. This is in agreement with the results found by Katayama and Ando.[13] They found the excitonic shift to be about 1 meV.

We now turn to Raman intensities. Figures 5(a) and 5(b) show the calculated intensity I versus ω, the energy loss of the scattered light for $qa=0.2$, 0.5, 0.7, and 1.0, at $2ka=5.8$, for a system with the same parameters as in Fig. 3, except that $N=15$. As q increases, one observes how the intrasubband peaks are passing the intersubband peak. Recently Pinczuk *et al.*[6] studied a superlattice, where they found the intrasubband peak at a higher energy than the intersubband peak. We have done calculations for a system with the same density and intersubband separation as the one studied by Pinczuk *et al.*, and we find that it is more likely that the intersubband peak is at a higher energy than the intrasubband peak. When a

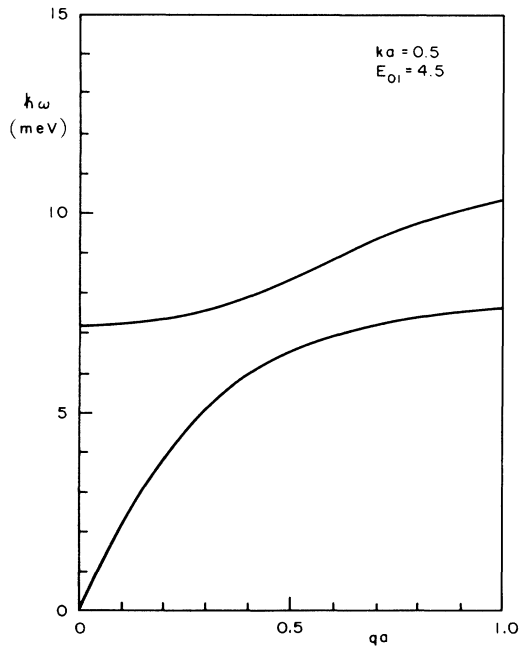

FIG. 4. Dispersion relation ω vs q for the $ka=0.5$ bulk intrasubband plasmon (infinite system). The parameters are the same as in Fig. 3.

magnetic field is applied parallel to the superlattice axis, the intrasubband plasmon increases in energy, while the energies of the intersubband modes are rather unaffected. This will then result in a crossing between intrasubband and intersubband modes at a finite magnetic field.

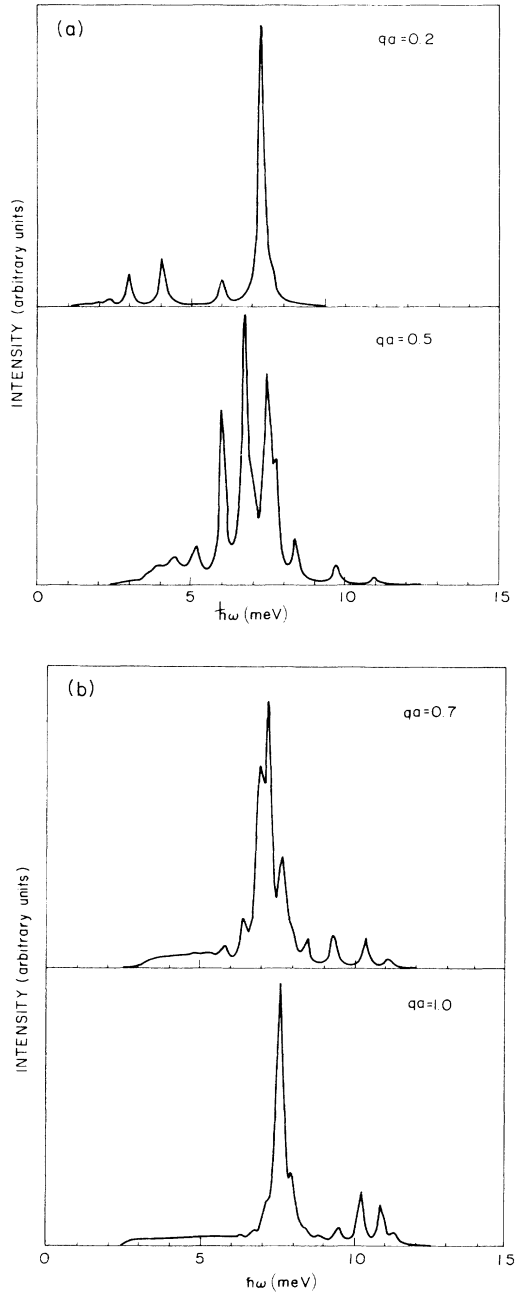

FIG. 5. (a) Raman intensities vs ω, the energy loss of the incoming photon at $qa=0.2$ and $qa=0.5$. The parameters are $n_s=8.2\times10^{11}$ cm^{-2}, $a=980$ Å, $L=350$ Å, $d_2=150$ Å, $\delta=0.6a$, $N=15$, $\gamma_e=\gamma_{\rm ph}=0.1$ meV. The intersubband separation is 4.5 meV. (b) Raman intensities vs the energy loss ω of the incoming photon, at $qa=0.7$ and $qa=1.0$. The parameters as in (a).

V. CONCLUSIONS AND DISCUSSION

In this paper we have calculated the density-density correlation function for a finite type-I superlattice, including finite width of the quantum wells, intersubband scattering, many-body effects such as exchange and correlation, and finite-size effects. We find that the finite size of the superlattice results in a discrete structure of the Raman intensity. The effects of exchange and correlations are found to be very small for intrasubband modes, and only minor for the intersubband modes in the form of a weak excitonic shift. We have demonstrated that intersubband scattering becomes very important when two or more subbands are occupied. Coupling between intersubband and intra-subband plasmons is also very important when the subband separation is of the same order as the intrasubband plasma frequency. This effect can be demonstrated experimentally: The variation of the in-plane momentum transfer q or the momentum transfer k along the superlattice axis will show the interchange of the intersubband and intrasubband modes. Some small broadening of the intrasubband resonances due to the intersubband single-particle excitations is also expected. Also, both the justification and the range of the validity of the layered electron gas model and the diagonal approximation has been given. We have assumed that the overlap of the electronic wave functions is negligible, thus assuming thick $Ga_{1-x}Al_xAs$ layers. For a system where the barriers are thin enough that this is no longer true, the theory above can be extended. Effects of a magnetic field applied parallel to the superlattice axis can also be taken into account, replacing χ^0 with a corresponding expression for an electron gas in magnetic field.

ACKNOWLEDGMENT

The authors would like to acknowledge financial support by the U.S. Army Research Office (Durham, NC).

APPENDIX A: CALCULATION OF WAVE FUNCTIONS

The procedure used here is essentially the same as described in Ando and Mori.[18] It assumes that the electron has approximately the same effective mass in the GaAs layers as in the $Ga_{1-x}Al_xAs$ layers. An approach that takes care of the actual differences in the effective mass in the two media is given by Ando.[23]

The one-electron wave function in a periodic potential satisfies the Schrödinger equation

$$-\frac{\hbar^2}{2m}\frac{d^2}{dz^2}\xi_{n,k_z}(z)+V(z)\xi_{n,k_z}(z)=E_n(k_z)\xi_{n,k_z}(z)\ , \qquad \text{(A1)}$$

where k_z is the Bloch wave vector, and n is the subband index,

$$V(z)=V_0\sum_{l=-\infty}^{\infty}\Theta((\tfrac{1}{2}L)^2-[z-(l-\tfrac{1}{2})a]^2) + v(z)+V^{\rm xc}(z) \qquad \text{(A2)}$$

is the potential well, and $v(z)$ is the Hartree potential

$$\frac{d^2}{dz^2}v(z)=-\frac{4\pi e^2}{\epsilon}\left[n(z)-\frac{aN_D}{d_1-2d_2}\sum_{l=-\infty}^{\infty}\Theta((\tfrac{1}{2}d_1+d_2)^2-[z-(l+\tfrac{1}{2})a]^2)\right]. \tag{A3}$$

The second term comes from the doping in the $Ga_{1-x}Al_xAs$ layers. A spacer layer of undoped $Ga_{1-x}Al_xAs$ with thickness separates the GaAs layer from the doped region. The doping ions are replaced by a uniform positive background with charge density N_D. $n(z)$ is the electron density distribution. In order to solve Eq. (A1), we write $\xi_{n,k_z}(z)$ as

$$\xi_{n,k_z}(z)=\frac{1}{\sqrt{a}}e^{ik_z a}\sum_{l=-\infty}^{\infty}c_l^{(n)}(k_z)e^{i\alpha_l z}, \tag{A4}$$

where $\alpha_l=2\pi l/a$. If the overlap between different wells is negligible, then the energies $E_n(k_z)$ are independent of k_z (flat minibands), we can write $\xi_{n,k_z}(z)$ in terms of the following Wannier functions:

$$\xi_{n,k_z}(z)=\sum_{l=-\infty}^{\infty}e^{ik_z la}\xi_n(z-la), \tag{A5}$$

where $\xi_n(z)$ is the wave function for a single cell. It is given by

$$\xi_n(z)=\frac{1}{\sqrt{a}}\sum_l c_l^{(n)}e^{i\alpha_l z}=\frac{1}{\sqrt{a}}\sum_l c_l^{(n)}(k_z=0)e^{i\alpha_l z}. \tag{A6}$$

In Fourier space Eq. (A1) is

$$\frac{\hbar^2}{2m}(k_z+\alpha_l)^2c_l^{(n)}(k_z)+\sum_{l'}V_{l-l'}c_{l'}^{(n)}(k_z)=E_n(k_z)c_l^{(n)}(k_z) \tag{A7}$$

where

$$V_l=-\frac{V_0}{\pi l}\sin\left[\frac{\pi lL}{a}\right]+\frac{4\pi e^2}{\epsilon}\left[n_l-\frac{aN_D}{d_1-2d_2}\frac{1}{\pi l}\sin\left[\frac{L}{2}+d_2\right]\right]+V_l^{xc}. \tag{A8}$$

The exchange-correlation potential used here is the same as used by Ando and Mori. It is used for calculating the ground state as well as the excited states. The expression has been parametrized by Gunnarson and Lungquist:[24]

$$V^{xc}=-\frac{2}{\pi\alpha}\left[\frac{1}{r_s}+0.545\ln\left[1+\frac{1.14}{r_s}\right]\right]\text{Ry}^*, \tag{A9}$$

where $\alpha=(4/9\pi)^{1/3}$ and

$$n(z)=\left[\frac{4\pi}{3}(a_B^* r_s)^3\right]^{-1}$$

and a_B^* and Ry^* are the effective Bohr radius and effective Rydberg. The matrix equation (A7) is truncated at $l=l_{\max}$ and solved iteratively for $k_z=0$. It converges fast (approximately ten iterations). Note that if the wave functions $\xi_n(z)$ are localized in quantum wells, they can be used as a very good approximation of the wave function in a finite system.

APPENDIX B: CALCULATION OF MATRIX ELEMENTS

The bulk and surface parts of $\underline{V}(k,k')$ are respectively,

$$\underline{V}_B(k)=V_q[\underline{g}_-(q)(e^{-ika}-e^{-qa})+\underline{g}_-(-q)(e^{ika}-e^{-qa})]/2P(k)+V_q\underline{g}^0(q)+U_{xc}, \tag{B1}$$

where

$$g_{\pm pp'}(q)=\int dz\int dz'\,\xi_m(z)\xi_n(z)\times e^{-q(z\pm z')}\xi_{m'}(z')\xi_{n'}(z'), \tag{B2}$$

$$g^0_{pp'}(q)=\int dz\int dz'\,\xi_m(z)\xi_n(z)\times e^{-q|z-z'|}\xi_{m'}(z')\xi_{n'}(z'), \tag{B3}$$

and

$$\underline{V}_S(k,k')=V_q\frac{1-e^{-qaN}}{4NP(k)P(k')}\times(\underline{a}-\underline{b}_1e^{ika}-\underline{b}_2e^{-ik'a}+\underline{c}e^{i(k-k')a}), \tag{B4}$$

$$\underline{a}=\underline{g}_-(q)+\underline{g}_-(-q)+\bar{\alpha}\underline{g}_+(q)e^{2qa}, \tag{B5}$$

$$\underline{b}_1=\underline{g}_-(q)e^{-qa}+\underline{g}_-(-q)e^{qa}+\bar{\alpha}\underline{g}_+(q)e^{qa}, \tag{B6}$$

$$\underline{b}_2=\underline{g}_-(q)e^{qa}+\underline{g}_-(-q)e^{-qa}+\bar{\alpha}\underline{g}_+(q)e^{qa}, \tag{B7}$$

$$\underline{c}=\underline{g}_-(q)+\underline{g}_-(-q)+\bar{\alpha}\underline{g}_+(q), \tag{B8}$$

$$\bar{\alpha}=(1-e^{-qaN})\alpha. \tag{B9}$$

The matrix M in Eq. (3.17) is given by

$$M=\begin{bmatrix}1-\underline{a}\cdot\underline{G}-\underline{b}_2\cdot\underline{H}_- & \underline{a}\cdot\underline{H}_+-\underline{b}_2\cdot\underline{G}\\ \underline{c}\cdot\underline{H}-\underline{b}_1\cdot\underline{G} & 1-\underline{c}\cdot\underline{G}+\underline{b}_1\cdot\underline{H}_+\end{bmatrix}, \tag{B10}$$

where

$$\underline{G}=\frac{1-e^{-qaN}}{4N}\sum_k\frac{1}{P(k)^2}\underline{\chi}_B(k), \tag{B11}$$

$$\underline{H}_{\pm}=\frac{1-e^{-qaN}}{4N}\sum_{k}\frac{e^{\pm ika}}{P(k)^2}\chi_B(k)\ . \tag{B12}$$

The wave functions $\xi_m(z)$ are given by the following Fourier expansions:

$$\xi_m(z)=\frac{1}{\sqrt{a}}\sum_{l=-\infty}^{\infty}c_l^{(m)}e^{i\alpha_l z}\ , \tag{B13}$$

where $\alpha_l=2\pi l/a$. The phases of $c_l^{(m)}$ are such that $\xi_m(z)$ are real functions. We notice that the parity of $\xi_m(z)$ is $(-1)^m$ if the overlap between the wells is negligible and the potential well is symmetric under spatial inversion. Defining

$$\tilde{g}_p(q)=\int dz\,\xi_m(z)\xi_n(z)e^{-qz}\ , \tag{B14}$$

we can express $\underline{g}_+(q)$ and $\underline{g}_-(q)$ in terms of $\tilde{g}$:

$$g_{-pp'}(q)=\tilde{g}_p(q)\tilde{g}_{p'}(q)(-1)^{n'+m'}\ , \tag{B15}$$

$$g_{+pp'}(q)=\tilde{g}_p(q)\tilde{g}_{p'}(q)\ . \tag{B16}$$

Defining

$$n_l^{(p)}=\sum_{l'}c_{l-l'}^{(m)}c_{l'}^{(n)}\ , \tag{B17}$$

we find

$$\tilde{g}_p(q)=2\sinh\left[\frac{qa}{2}\right]\left[2\sum_{l=1}^{\infty}(-1)^l\mathrm{Re}\left[\frac{n_l^{(p)}}{qa-2\pi il}\right]+\frac{n_0^{(p)}}{qa}\right]. \tag{B18}$$

$g_{pp'}^0(q)$ finally is

$$g_{pp'}^0=2qa\sum_{l=0}^{\infty}\frac{n_l^{(p)}n_l^{(p')}}{(qa)^2+4\pi^2l^2}$$
$$-2(1-e^{-qa})[(qa)^2h_1^{(p)}h_1^{(p')}-4\pi^2h_2^{(p)}h_2^{(p')}]\ , \tag{B19}$$

where

$$h_1^{(p)}=\frac{n_0^{(p)}}{(qa)^2}+2\sum_{l=1}^{\infty}(-1)^l\frac{\mathrm{Re}(n_l^{(p)})}{(qa)^2+4\pi^2l^2}\ , \tag{B20}$$

$$h_2^{(p)}=2\sum_{l=1}^{\infty}(-1)^l l\frac{\mathrm{Im}(n_l^{(p)})}{(qa)^2+4\pi^2l^2}\ . \tag{B21}$$

[1] L. Esaki, in *Proceedings of the 17th International Conference on the Physics of Semiconductors, San Fransisco, 1984,* edited by J. D. Chadi and W. A. Harrison (Springer, New York, 1985), p. 473.

[2] D. Olego, A. Pinczuk, A. Gossard, and W. Wiegmann, Phys. Rev. B **25**, 7867 (1982).

[3] R. Sooryakumar, A. Pinczuk, A. Gossard, and W. Wiegmann, Phys. Rev. B **31**, 2578 (1985).

[4] G. Fasol, N. Mestres, H. P. Hughes, A. Fischer, and K. Ploog, Phys. Rev. Lett. **56**, 2517 (1986).

[5] A. Pinczuk, M. G. Lamont, and A. C. Gossard, Phys. Rev. Lett. **56**, 2092 (1986).

[6] A. Pinczuk, D. Heiman, A. C. Gossard, and J. H. English, *Proceedings of the 18th International Conference on the Physics of Semiconductors, Stockholm, 1986* (World-Scientific, Singapore, in press).

[7] E. Burstein, A. Pinczuk, and D. L. Mills, Surf. Sci. **98**, 451 (1980).

[8] A. Tselis and J. J. Quinn, Phys. Rev. B **29**, 3318 (1984).

[9] S. Das Sarma, Phys. Rev. B **29**, 2334 (1984).

[10] G. F. Giuliani and J. J. Quinn, Phys. Rev. Lett. **51**, 919 (1983).

[11] P. Hawrylak, J.-W. Wu, and J. J. Quinn, Phys. Rev. B **31**, 7855 (1985).

[12] J. K. Jain and P. B. Allen, Phys. Rev. Lett. **54**, 947 (1984); Phys. Rev. B **32**, 997 (1985).

[13] S. Katayama and T. Ando, J. Phys. Soc. Jpn. **54**, 1615 (1985).

[14] R. D. King-Smith and J. C. Inkson, Phys. Rev. B **33**, 5489 (1986).

[15] P. Hawrylak, J.-W. Wu, and J. J. Quinn, Phys. Rev. B **32**, 5169 (1985).

[16] N. Tzoar and C. Zhang, Phys. Rev. B **34**, (1986).

[17] P. Hawrylak, G. Eliasson, and J. J. Quinn, Phys. Rev. B **34** (1986).

[18] T. Ando and S. Mori, J. Phys. Soc. Jpn. **47**, 1518 (1979).

[19] F. Stern, Phys. Rev. Lett. **18**, 546 (1967).

[20] P. Hawrylak, J.-W. Wu, and J. J. Quinn, Phys. Rev. B **32**, 4272 (1985).

[21] P. Hawrylak and J. J. Quinn, Phys. Rev. B **33**, 8264 (1986).

[22] P. Hawrylak, Phys. Rev. B **35**, 3818 (1987).

[23] T. Ando, J. Phys. Soc. Jpn. **51**, 3893 (1982).

[24] O. Gunnarson and B. I. Lundquist, Phys. Rev. B **13**, 4274 (1976).